ELECTROMAGNETIC STIRRING OF STEEL: EFFECT OF STIRRER DESIGN ON MIXING IN HORIZONTAL ELECTROMAGNETIC STIRRING OF STEEL SLABS

N. El-KADDAH[1] and T.T. NATARAJAN[2]

[1] Department of Metallurgical and Materials Engineering
The University of Alabama, Tuscaloosa, AL 35487-0202 USA

[2] U.S. Steel Tech Center, Monroeville, PA 15146 USA

ABSTRACT

Electromagnetic stirring is widely used in continuous casting of steel as a means to improve homogeneity of cast slabs. Industrial experience has shown that stirrer design and operating conditions have a strong influence on the metallurgical quality of the cast slab. This paper examines the effect of the stirrer current and field frequency on the flow in horizontal EMS of steel slabs. A three-dimensional model for computing the electromagnetic and velocity fields in continuous casting systems is presented. The stirrer current and frequency were found to affect the primary horizontal flow in the vertical section covered by the stirrer and to have a significant effect on the upward flow in the force-free region above the edges of the stirrer. It was also found that flow is quite turbulent in the region facing the stirrer, and turbulent mixing diminishes rapidly beyond the edges of the stirrer. It has also been demonstrated that through changes in the stirrer current and/or field frequency, it is possible to modify the magnitude and distribution of turbulent characteristics of the induced flow.

NOMENCLATURE

D   deformation tensor
F_{em} Lorentz force
H   magnetic field intensity
I   stirrer current
J   current flux density
k   turbulent kinetic energy
P   pressure
T   current vector potential
U   velocity
ε turbulent energy dissipation
μ_o magnetic permeability
μ_l laminar viscosity
μ_t turbulent viscosity
ρ density
σ electrical conductivity
ϕ phase shift
Ψ reduced magnetic scalar potential
ω frequency

INTRODUCTION

In recent years most steel producers have recognized that control of fluid flow and mixing phenomena in continuous casters is necessary to improve the overall quality of cast billets and slabs. More specifically, it has been appreciated that in addition to reducing solute segregation during solidification, the flow may play a key role in eliminating inclusions, blowholes and center porosity. As a result, electromagnetic stirring (EMS) has become an integral component of the continuous casting process (Birat and Chone, 1982; Kollberg, 1980).

In EMS of billets and slabs, induction stirrers are placed in the mold, below the mold, and/or in the final solidification zone depending on metallurgical objectives. For slab casting, melt stirring is accomplished using linear stirrers of finite height. These stirrers can be regarded as induction motor stators producing traveling a magnetic field, which generates a force field in the strand, resulting in a recirculating flow field in the molten pool. It is generally accepted that the maximum velocities have to be in excess of about 0.2 ~ 0.5 m/s for the stirring to be effective, although these limits are not firmly established.

During the past decade a considerable effort has been made to develop a quantitative description of the electromagnetic and flow phenomena in sub-mold stirring of slabs. The early work by Dubke *et al*. (1988) and Saluja *et al*. (1990) employed an approximate two-dimensional analytical expression for the force field. The most recent efforts have made use of numerical techniques for the solution of Maxwell's equations to describe the field in terms of the stirrer geometry and the stirrer current and frequency (Meyer *et al*., 1987; Natarajan and El-Kaddah, 1998). As a result of this latter work, one may now, with some confidence, quantitatively predict the electromagnetic and velocity fields for any given stirrer configuration and operating conditions. The purpose of this paper is to investigate the effect of stirrer current and frequency on the induced flow in sub-mold horizontal EMS of slabs.

FORMULATION

The mathematical description of the EMS system involves the solution of Maxwell's equations to determine the induced force field in the slab, and the turbulent Navier-Stokes equations together with turbulent-model equations to calculate the velocity field in the molten pool. It is assumed that the thickness of the solidified shell in the solution domain is infinitesimally small. It is also assumed that the flow in the molten pool due to pouring does not affect the electromagnetically induced flow. This assumption is

reasonable as the inertial flow produced by the incoming molten metal stream is generally confined to the mold region.

Electromagnetic Field Equations

The unique feature of the model described here is in its description of the electromagnetic field in terms of potentials to avoid discontinuity of the electric field at boundaries of the slab. In this work, the electric current density, J, and the magnetic field intensity, H, are formulated using current vector potential, T ($J = \nabla \times T$), and the reduced magnetic scalar potential, Ψ ($H = T - \nabla \Psi$).

From Maxwell's equations, the differential equations describing T and Ψ in a medium with a constant electrical conductivity subjected to a time harmonic applied magnetic field of frequency ω, generated by an induction coil are:

$$\nabla^2 T = -j\sigma\omega\mu_o \left(T - \nabla\Psi \right) \qquad (1)$$

$$\nabla^2 \Psi = 0 \qquad (2)$$

where $j = \sqrt{-1}$ and σ and μ_o are the electrical conductivity and magnetic permeability of the metal, respectively.

The boundary conditions for the T equation, which enforces zero current across the outer surface of the strand is given by:

$$T_i = 0 \qquad \forall i = 1,3 \qquad (3)$$

In order to incorporate complicated coil configuration into the model formulation, the boundary condition on Ψ at the surface of the metal is expressed by Biot-Savart's law, which may be written as:

$$\nabla\Psi \cdot n = \left[T - \left(\frac{1}{4} \left(\sum_{coil} I\, e^{j\phi} \int \frac{dl \times (r\text{-}r')}{|r\text{-}r'|^3} + \sum_{slab} \int_e \frac{(\nabla \times T) \times (r\text{-}r')}{|r\text{-}r'|^3} dV \right) \right) \right] \cdot n \quad (4)$$

where I and ϕ are the amplitude and phase shift of the multiphase current in each coil turn, dl is an element of length along the coil turn, dV is a volume element in the metal, and |**r-r'**| is the distance from a point in the metal to the respective integration element.

The first and second terms in equation (4) describe the applied magnetic field resulting from the stirrer and the induced field in the slab, respectively. The form of the integral for the applied field is such that the location and current of each stirrer turn may be individually specified. This means that the model is very flexible to investigate the induced flow for any given stirrer configuration and stirrer current.

Finally, the time averaged electromagnetic force in the conductor can be described in terms of T and Ψ by the following equation:

$$\mathbf{F}_{em} = \frac{\mu_0}{2} \mathrm{Re}((\nabla \times \mathbf{T}) \times (\mathbf{T} - \nabla\Psi)^*) \qquad (5)$$

where the asterisk denotes the complex conjugate.

Fluid Flow Equations

Within the framework of the assumptions stated at the beginning of this section, the governing equation describing the flow in the molten pool takes the following form:

Conservation of mass:

$$\nabla \cdot \left(\rho U \right) = 0 \qquad (6)$$

Turbulent Navier-Stokes equation:

$$\rho(U \cdot \nabla)U = -\nabla p - \left[\nabla \cdot (\mu_i + \mu_t)D \right] + F_{em} \qquad (7)$$

where

$$D_{ij} = \left(\frac{\partial U_i}{\partial x_j} + \frac{\partial U_j}{\partial x_i} \right) \qquad \forall i, j = 1,3$$

D is the deformation tensor, **U** is the time averaged velocity vector, ρ is fluid density, p is the pressure in the fluid, and μ_l and μ_t are the laminar and turbulent viscosity, respectively.

The k-ε turbulent model:

The turbulent viscosity, μ_t, in this model is given by:

$$\mu_t = c_\mu \frac{\rho k^2}{\varepsilon} \qquad (8)$$

where k is the turbulent kinetic energy, and ε is turbulent energy dissipation, and C_μ is a constant. The differential equations for k and ε are given by:

$$\rho(U \cdot \nabla)k = \nabla \cdot \left(\frac{\mu_t}{\sigma_k} + \mu_l \right) \nabla k + G - \rho\varepsilon \qquad (9)$$

$$\rho(U \cdot \nabla)\varepsilon = \nabla \cdot \left(\frac{\mu_t}{\sigma_\varepsilon} + \mu_l \right) \nabla\varepsilon + c_1 \frac{\varepsilon}{k} G - c_2 \rho \frac{\varepsilon^2}{k} \quad (10)$$

where

$$G = \mu_t D_{ij} \frac{\partial U_i}{\partial x_j}$$

G is the rate of generation of turbulence, and c_1, c_2, σ_k, σ_e and c_μ are constants.

Equations (1-10) together with appropriate boundary conditions, which are not reproduced here for sake of brevity, represent the complete statement of the problem. These equations were discretized using the finite element method. Details of the finite element formulation and solution technique are in the paper by Natarajan and El-Kaddah (1998).

RESULTS AND DISCUSSION

In this study, we investigated the effect of the operating conditions of a typical 3-phase linear stirrer on the induced flow in a 2000x250-mm slab. Calculations were performed for the stirring arrangement shown in Figure 1. The velocity data was generated for stirrer currents of 2400 and 3200 A at frequencies of 10 and 20 Hz. The system parameters used in these calculations are

summarized in Table I, while the physical property data of steel is given in Table II.
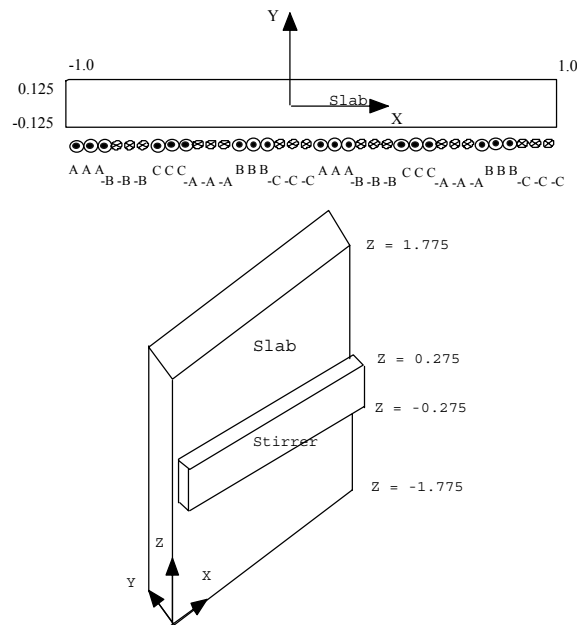

Figure 1. Sketch of the EMS system

Table I. System Parameters

Dimensions of the slab	2000 x 250 mm
Dimensions of the stirrer	2000 x 550 mm
Distance from slab to stirrer	60 mm
Number of phases	3
Number of pairs of poles	2
Number of turns per phase per pole	3
Polar pitch	500 mm
Current amplitude per phase	2400 - 3200 A
Frequency	10-20 Hz

Table II. Physical Properties of Steel

Density	7.0×10^3 Kg/m^3
Laminar viscosity	6.3×10^{-3} Kg m/s
Electrical conductivity	7.7×10^5 mhos/m

In the following we shall present a selection of computed plots, with emphasis on providing a general understanding of the rather complex three-dimensional flow that occurs in horizontal EMS of slabs, and the effect of the stirrer current and frequency on the flow field. Essentially two types of results will be presented, namely, velocity maps and contour plots of the turbulent intensity.

Figure 2 shows a typical computed tracer particle trajectory in the melt, where it is seen that the flow field exhibits the characteristic two recirculating loops characteristic of horizontal EMS of slabs. This figure shows that the flow in the vertical section covered by the stirrer, which is driven by electromagnetic forces, is predominantly horizontal, and the recirculating flow

beyond the stirrer appears to be caused by the deflection of the primary flow at the west wall of the slab (x=-1.0).
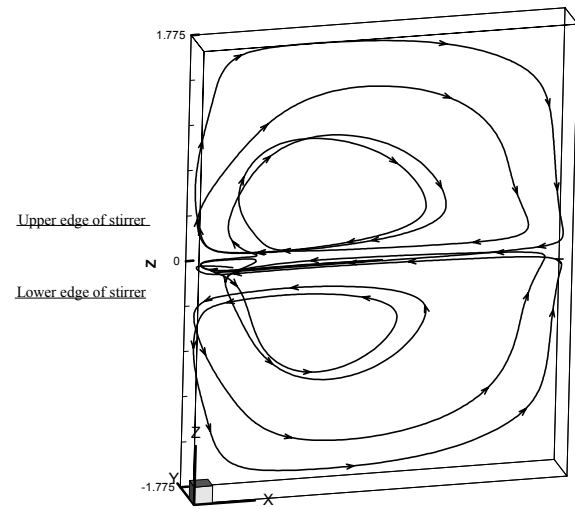

Figure 2. Computed flow pattern

The velocity field in the stirrer region is depicted in Figure 3, which shows the computed velocity vectors in the horizontal x-y plane at the center of the stirrer (y=0). It is seen that, as perhaps expected, the flow accelerates along the slab from zero velocity at the east wall (x=1) to its steady velocity in the middle of the slab (x=0). This figure also shows a strong swirling flow near the west wall. The induced flow along the slab before the swirl (x >-0.5) is essentially one-dimensional in the direction of the traveling magnetic field, i.e. the x-direction. In addition, it is non-uniform across the slab with a maximum velocity near the wall facing the stirrer and a minimum in the opposite side of the slab, which can not be avoided in linear EMS due to the decay of the electromagnetic force field in the skin depth.
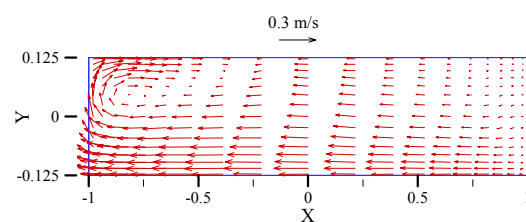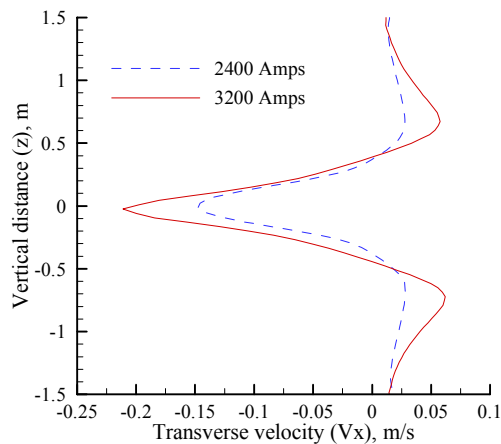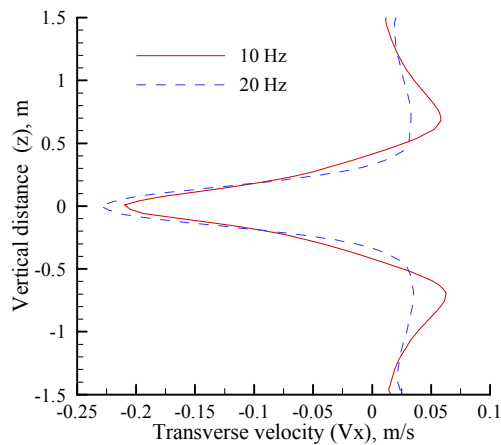

Figure 3. Velocity vector plot in x-y plane at z=0: I=3200 A, f=10Hz

The effect of stirrer operating parameters on the steady flow along the slab is illustrated in Figures 4 and 5, which show the computed profile of transverse velocity V_x at the center of the slab (x=0, y=0). Figure 4 represents the influence of changing the stirrer current at fixed field frequency, while Figure 5 depicts the velocity profiles at different frequencies. These figures show that the transverse velocity is a maximum at the center of the stirrer (z=0), and the velocity profile depends on both the stirrer current and frequency. Inspection of Figure 4 shows that the maximum velocity varies linearly with the coil current. Although the frequency has little effect on
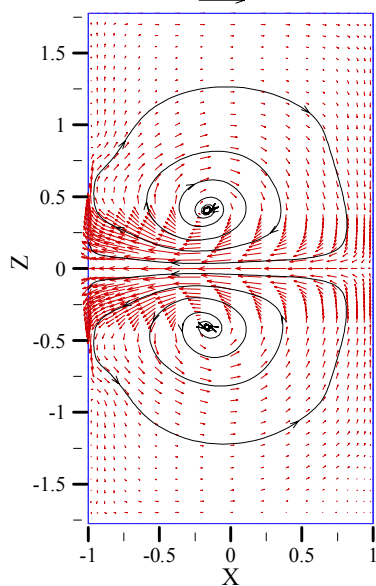
the magnitude of the maximum velocity, it does affect the recirculating flow pattern in the molten pool.

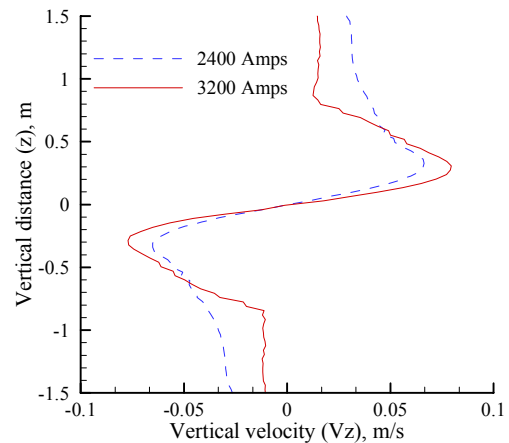**Figure 4**. Effect of stirrer current on the transverse velocity: x=0; y=0; f= 10 Hz

Figure 5. Effect of field frequency on the transverse velocity: x=0; y=0; I=3200 A
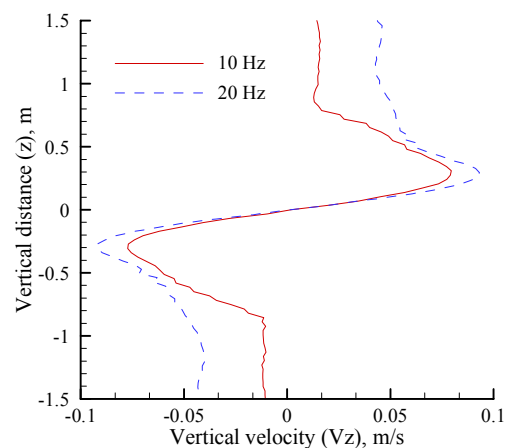

Figure 6. Velocity vector plot in x-z plane at y=0: I=3200 A, f=10 Hz

The circulation of the primary horizontal flow in the molten pool beyond the stirrer is illustrated in the velocity plot in the x-z plane, Figure 6. This figure clearly shows that the flow beyond the stirrer is caused by the deflection of the horizontal flow at the west wall. The recirculating flow brought about by the upward flow extends almost to the other end of the slab even though the streamline velocities are an order of magnitude smaller than the mean velocity of the primary flow.

Since the inertia of the upward flow sustains the flow in unforced regions, one may use the upward velocity as a measure of the penetration of the flow in the molten pool. Figure 7 and 8 shows the computed profiles of velocity component V_z near the wall for the cases considered in this study. Inspection of these figures shows that the regions of highest velocity correspond to the edges of the stirrer, and the effective stirring region, where the velocity is significant, is about three times the height of the stirrer. Furthermore, the stirrer current and frequency have little effect on the maximum velocity, but strongly affect the penetration of upward flow in the molten pool.

Figure 7. Effect of stirrer current on the vertical velocity: x=-0.95 m; y=0; f= 10 Hz

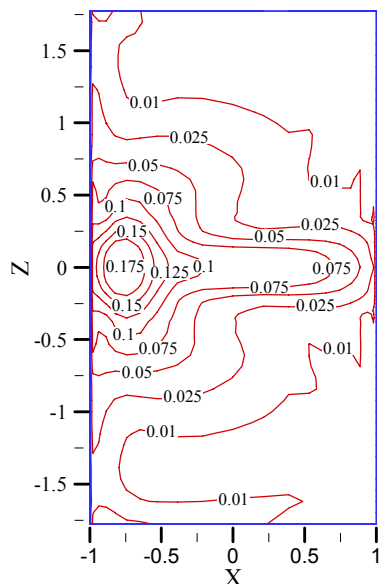
Figure 8. Effect of field frequency on the vertical velocity: x=-0.95 m; y=0; I= 3200 A

The velocity vector plots provide useful insight into the complexities of the flow patterns in the horizontal EMS of slabs. Additional important insights may be obtained by considering the turbulent behavior, depicted in Figures 9, 10 and 11. Turbulence is important in EMS because it will aid mixing and homogenization of the molten pool.
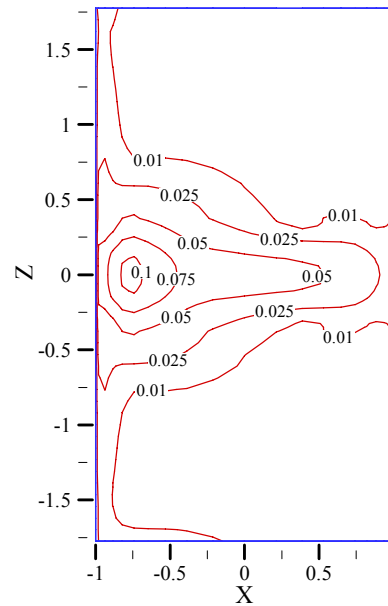
Figure 9 shows the computed turbulent intensity (turbulent kinetic energy k normalized with respect to the mean velocity, 0.3 m/s) in the vertical x-z plane for stirrer current of 3200 A and frequency of 10 Hz. It is seen that significant levels of turbulence will exist throughout the molten pool with maximum intensity of 0.175 in the vicinity of the west wall. With the exception of this region, the turbulent intensity of the primary flow is significantly small, about 0.05. The turbulent intensity of the recirculating flow beyond the stirrer is even smaller: too small to play a significant role in promoting melt homogenization and temperature uniformity.

Figure 10 shows the corresponding plot, but at lower current of 2400 A. The turbulent structure is identical to that at higher current described above. However, the flow is less turbulent than the previous case, and the maximum turbulent intensity is about 0.1. This decrease is expected due to the decrease of melt velocities by reducing the coil current. The results suggest that the turbulent intensity is directly proportional to the stirrer current.
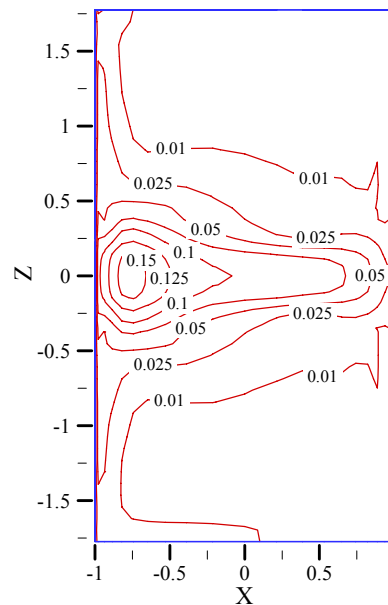
Figure 11 shows the effect of increasing the frequency to 20 Hz for a stirrer current of 3200 A. Qualitatively there is no significant change in the turbulent field from that obtained for 10 Hz. The computed turbulent intensity is slightly smaller than that for 10 Hz by about 10%.

Figure 10. Turbulent intensity plot in x-z plane at y=0: I=2400 A, f=10 Hz

Figure 11. Turbulent intensity plot in x-z plane at y=0: I=3200 A, f=20 Hz

The parametric study presented here has elucidated the role of the stirrer current and frequency on the flow and turbulent mixing in horizontal EMS of slabs. Although the findings of this work are limited to the input parameters and coil configuration used, the model presented in this paper is a general one and can be used for determining the operating conditions for all types of induction stirrers used in continuous casting of steel.

Figure 9. Turbulent intensity plot in x-z plane at y=0: I=3200 A, f=10 Hz

CONCLUSIONS

A mathematical formulation and computed results are presented to describe the three-dimensional electromagnetic field, velocity field and turbulent parameters in horizontal EMS of slabs. The design and operating data of the stirrers used in the calculations are thought to be typical of those employed in continuous casting practice. The principal findings for linear stirring of slabs are that the electromagnetic force field is truly three dimensional, and the end effects of the stirrer cannot be ignored in the analysis of the flow. Furthermore, the flow in the central region of the stirrer is non-symmetrical with pronounced velocity and turbulent intensity gradients both along and across the width of the slab. While linear stirring induces flow in the molten pool beyond the region facing the stirrer, the velocity and turbulence were found to be too small to have a significant effect on mixing characteristics and solidification kinetics in that region. It was found that the stirring velocity increases linearly with increasing stirrer current and reducing the frequency enhances turbulent mixing in the melt. Finally, the model presented in this paper provides a theoretical framework for comprehensive modeling of electromagnetic, velocity, and heat transfer phenomena in the continuous casting process.

REFERENCES

BIRAT, J.P and CHONE, J., (1983) "Electromagnetic Stirring on Billet, Bloom, and Slab Continuous Casters: State of the Art in (1982)," *Ironmaking and Steelmaking*, **6**, 269-281.

DUBKE, M., TACKE, K., SPITZER, K. and SCHWERDTFEGER, K., (1988) "Flow Fields in Electromagnetic Stirring of Rectangular Strands with Linear Inductors: Part I. Theory and Experiments with Cold Models*," Metallurgical Transactions*, **19B**, 581-593.

DUBKE, M., TACKE, K., SPITZER, K. and SCHWERDTFEGER, K., (1988) "Flow Fields in Electromagnetic Stirring of Rectangular Strands with Linear Inductors: Part II. Computation of Flow Fields in Billets, Blooms, and Slabs of Steel*," Metallurgical Transactions*, **19B**, 595-602.

KOLLBERG, S., (1980) "Contribution to the Theory and Experience of Electromagnetic Stirring in Continuous Casting," *Iron and Steel Engineer*, **57**, 46-54.

MEYER, J.L., SZEKELY, J. and EL-KADDAH, N., (1987) "Calculation of the Electromagnetic Force Filed for Induction Stirring in Continuous Casting," *Transactions of ISIJ*, **27**, 25-33.

NATARAJAN, T.T. and EL-KADDAH, N., (1998) "Finite Element Analysis of Electromagnetically driven Flow in Sub-Mold Stirring of Steel Billets and Slabs," *ISIJ International*, **38**, 680-689.

SALUJA N., ILEGBUSI O.J. and SZEKELY, J., (1990) "Three-dimensional Flow and Free Surface Phenomena in Electromagnetically Stirred Molds in Continuous Casting," *Proceedings of the Sixth International Iron and Steel Congress*, ISIJ, **3**, 338-346.